Developmental Cell, Vol. 9, 757–767, December, 2005, Copyright ©2005 by Elsevier Inc. DOI 10.1016/j.devcel.2005.10.009

EBF2 Regulates Osteoblast-Dependent Differentiation of Osteoclasts

Matthias Kieslinger,[1,4] Stephanie Folberth,[1,4] Gergana Dobreva,[1,4] Tatjana Dorn,[1] Laura Croci,[3] Reinhold Erben,[2,5] G. Giacomo Consalez,[3] and Rudolf Grosschedl[1,4,*]

[1] Gene center and Institute for Biochemistry
University of Munich
81377 Munich
Germany

[2] Institute of Animal Physiology
University of Munich
80539 Munich
Germany

[3] San Raffaele Scientific Institute
20132 Milan
Italy

Summary

Communication between bone-depositing osteoblasts and bone-resorbing osteoclasts is required for bone development and homeostasis. Here, we identify EBF2, a member of the early B cell factor (EBF) family of transcription factors that is expressed in osteoblast progenitors, as a regulator of osteoclast differentiation. We find that mice homozygous for a targeted inactivation of *Ebf2* show reduced bone mass and an increase in the number of osteoclasts. These defects are accompanied by a marked downregulation of the *osteoprotegerin (Opg)* gene, encoding a RANK decoy receptor. EBF2 binds to sequences in the *Opg* promoter and transactivates the *Opg* promoter in synergy with the Wnt-responsive LEF1/TCF:β-catenin pathway. Taken together, these data identify EBF2 as a regulator of RANK-RANKL signaling and osteoblast-dependent differentiation of osteoclasts.

Introduction

The bones of vertebrates are formed and maintained by the interplay of different cell types. The bone-forming osteoblasts, which share a mesenchymal precursor with chondrocytes, secrete the bone extracellular matrix (ECM), whereas osteoclasts, which differentiate from hematopoietic progenitors of the myelomonocytic cell lineage, degrade the bone matrix (Karsenty and Wagner, 2002; Teitelbaum and Ross, 2003; Baron, 2004). During development, bone formation is initiated by the condensation of mesenchymal cells that differentiate along the chondrocytic pathway to form cartilage, which is subsequently replaced by bone, generated by osteoblasts in a process termed endochondral ossification. Alternatively, condensed mesenchymal cells can differentiate directly into osteoblasts to form intramembranous skeletal elements (de Crombrugghe et al., 2001; Olsen et al., 2000). The formation and maintenance of bones involves a fine balance between osteoblasts and osteoclasts, whereby osteoblasts regulate the differentiation of osteoclast precursors into terminally differentiated cells (Takahashi et al., 1988). Changes in the numbers and/or activities of osteoblasts and osteoclasts can result in an increase of bone mass, due to a failure of bone resorption (osteopetrosis) or increased bone production (osteosclerosis), or, alternatively, in a loss of bone mass, termed osteopenia or osteoporosis (Teitelbaum, 2000).

The communication between osteoblasts and osteoclasts is governed by at least two signaling pathways. The macrophage colony-stimulating factor (M-CSF) is secreted from osteoblasts and provides a survival signal to osteoclast precursors and osteoclasts (Lagasse and Weissman, 1997; Tsurukai et al., 2000; Yoshida et al., 1990). In addition, the tumor necrosis factor-related receptor activator of NF-κB ligand (RANKL), which is displayed on the cell surface of preosteoblasts and osteoblasts, regulates the differentiation of preosteoclasts by the interaction with the receptor activator of NF-κB (RANK) (Dougall et al., 1999; Kong et al., 1999; Lacey et al., 1998; Yasuda et al., 1998). Signaling by RANKL can be modulated by the decoy receptor Osteoprotegerin (OPG), which binds RANKL and is secreted from osteoblasts and several other cell types (Simonet et al., 1997). The role of OPG in regulating osteoclast differentiation and bone homeostasis was shown by targeted gene inactivation of the *Opg* gene, which results in enhanced osteoclast formation and osteoporosis (Bucay et al., 1998), and by the transgenic overexpression of *Opg*, which results in osteopetrosis (Simonet et al., 1997).

Several transcription factors have been shown to regulate the differentiation and function of osteoblasts and osteoclasts. Differentiation of osteoblasts, which can be monitored by the expression of markers such as *alkaline phosphatase*, *bone sialoprotein*, and *osteocalcin*, is regulated by the transcription factors Runx2/Cbfa1 and Osterix. *Runx2* is expressed at the onset of osteoblast differentiation (Ducy et al., 1997), and targeted disruption of this gene results in a complete absence of osteoblasts (Komori et al., 1997; Otto et al., 1997). Likewise, the genetic inactivation of *Osterix* leads to an arrest of osteoblast differentiation (Nakashima et al., 2002). In addition, the transcription factors ATF4 and TCF1 regulate the function of osteoblasts, which includes the differentiation of osteoclasts (Glass et al., 2005). This process is also regulated by transcription factors that act in the monocyte/myeloid lineage, such as Pu.1 (Tondravi et al., 1997), NFATc, NF-κB, and the AP1 proteins *c-fos* and *c-jun*, which function downstream of RANKL signaling (Kenner et al., 2004; Takayanagi et al., 2002a, 2002b). Although the role of the RANK-RANKL signaling pathway in the osteoblast-mediated differentiation of osteoclasts has been well established, our insight into the transcriptional control mechanisms that operate upstream of this signaling pathway is limited.

*Correspondence: grosschedl@immunbio.mpg.de

[4] Present address: Max-Planck Institute of Immunobiology, 79108 Freiburg, Germany.

[5] Present address: Department of Natural Sciences, University of Veterinary Medicine, 1210 Vienna, Austria.

Transcription factors of the "early B cell factor" (EBF) family bind to DNA as homo- or heterodimers through a zinc finger domain and a helix-loop-helix-like dimerization domain (Dubois and Vincent, 2001). The founding member of this family, EBF1, is expressed in B lymphocytes, adipocytes, and neuronal cells, and targeted inactivation of the *Ebf1* gene results in a block of early B cell differentiation (Hagman et al., 1993; Lin and Grosschedl, 1995). Other family members, including EBF2 (O/E3) and EBF3 (O/E2), are expressed in adipocytes, neurons, and several other cell types (Garel et al., 1997; Malgaretti et al., 1997; Mella et al., 2004; Wang et al., 2004). EBF proteins can act in a redundant manner, but some functions have been attributed to specific members of the family (Corradi et al., 2003; Wang et al., 2004). *Ebf2* is expressed in the embryonic central nervous system (Malgaretti et al., 1997), and targeted gene inactivation of *Ebf2* has revealed an important function in peripheral nerve morphogenesis, the migration of neurons that produce gonadotropin-releasing hormone, and projections of olfactory neurons (Corradi et al., 2003; Wang et al., 2004). However, the role of EBF2 in other developmental processes has not been studied. In this study, we show that EBF2 is also expressed in osteoblastic progenitors and regulates osteoclast differentiation by activating the gene encoding the RANK decoy receptor OPG.

Results

Expression of EBF2 in Osteoblastic Precursors

With the aim of examining the developmental expression pattern of EBF2 in more detail, we analyzed mice that carry an in-frame insertion of the bacterial *LacZ* gene immediately downstream of the translation initiation site of the *Ebf2* gene (Corradi et al., 2003). Whole-mount staining for β-galactosidase activity at different developmental stages showed that EBF2-lacZ is initially expressed in the first and second branchial arches at E9, in somites, specifically the forming sclerotomes, at E10 and E10.5, as well as in dorsal root ganglia at E12.5 (Figure S1; see the Supplemental Data available with this article online). Cryosections of E16.5 embryos revealed that EBF2 is expressed in bone-forming areas and adipose tissue (Figure 1A). Moreover, EBF2 is expressed in specific neural tissues, as described previously (Corradi et al., 2003). A similar expression pattern was observed in homozygous mutant embryos, indicating that the inactivation of the *Ebf2* gene does not result in a loss of EBF2-expressing cells (Figure 1B). In bone-forming areas, EBF2 is expressed along the mesenchymal condensations at E14.5 (Figure 1C), in the perichondrium, and in cells invading the cartilagenous structures at E16.5 (Figure 1D). In situ hybridization of tibias of E18.5 embryos to detect *Ebf2* transcripts indicated that individual *Ebf2*-expressing cells are scattered throughout the trabecular/cancellous bone area of wild-type mice, whereas no *Ebf2* transcripts can be detected in the corresponding areas of $Ebf2^{-/-}$ mice, which were used as a negative control (Figures 1E and 1F).

Various cell types, including osteoblasts and macrophages, are attached to the bone. To characterize the identity of the EBF2-expressing cells in more detail, we isolated adherent and nonadherent bone marrow cells from long bones of $Ebf2^{+/-}$ neonatal mice, by using collagenase and dispase, incubated the cells with anti-CD45 antibody, and loaded the cells with the fluorogenic β-galactosidase substrate FDG. In flow cytometry analysis, approximately 8% of the gated nonhematopoietic cells were positive for LacZ activity, and all of the CD45-positive hematopoietic cells were negative for EBF2-lacZ (Figure 1G and data not shown). Real-time RT-PCR analysis indicated that the EBF2-lacZ-expressing cells contain high levels of *Runx2* and low levels of *Sox9* transcripts (Figure 1H). These cells also contained low levels of transcripts of *alkaline phosphatase* and *bone sialoprotein*, but no detectable transcripts of *Osterix* and *osteocalcin*. Moreover, EBF2-lacZ-expressing cells contained transcripts of the chondrocyte marker *collagen2a1*, but lacked transcripts of other markers of chondrocytes (Figure S2A). We also analyzed the expression of EBF2 in sorted chondrocytes and in differentiated osteoclasts. Neither chondrocytes nor osteoclasts were found to express *Ebf2* (Figure S2A; data not shown). Finally, we examined the presence of EBF2-expressing cells in calvarial bone preparations of E18.5 $Ebf2^{+/-}$ mice by FDG loading and flow cytometry. We found that 2%–3% of the cells were positive for EBF2-lacZ (Figure S2B). Based on the expression of *Runx2*, the absence of *osteocalcin* transcripts, and the presence of low levels of *Sox9* and *collagen2a1* transcripts, EBF2-expressing cells appear to represent immature osteoblastic cells.

With the aim of further defining the expression of *Ebf2* in osteoblastic cells, we performed in vitro differentiation experiments with calvarial cells from newborn wild-type mice (Bellows et al., 1990). In this experiment, we placed calvarial cells of E18.5 wild-type mice into culture for 3 days and thereafter differentiated the cells into mature osteoblasts by the addition of β-glycerophosphate and ascorbic acid. Quantitative RT-PCR analysis of three independent cultures indicated that the expression of *Ebf2* is induced ~5-fold within 2 days, but declines after 4 days, when transcripts of *Osterix* and *osteocalcin* are detected at high levels (Figure 2A). *Ebf3* showed a similar profile of expression, albeit at a lower level, whereas transcripts of *Ebf1* accumulate in a pattern that resembles more that of *Osterix*. Taken together, these data suggest that *Ebf2* is expressed in immature osteoblastic cells that may include osteochondroprogenitor cells (Eames et al., 2004). Moreover, EBF2 may be partially redundant with other members of the EBF family of transcription factors.

Normal Bone Formation, but Low Bone Mass and High Bone Resorption, in $Ebf2^{-/-}$ Mice

To examine the consequences of a loss of EBF2 function on skeletal development, we performed alcian blue and alizarin red staining of skeletons at E18.5. No obvious differences in the morphology of bones and cartilages were detected between wild-type and $Ebf2^{-/-}$ mice (Figure 2B). Von Kossa staining and in situ hybridizations with probes to detect markers for osteoblasts (*bone sialoprotein*, *collagen1a1*) or chondrocytes (*collagen2a1*) did not reveal any significant changes in mutant embryos (Figure 2C). Moreover, histomorphometric analysis indicated that the cancellous bone area (B.Ar./T.Ar.) in the distal femurs of E18.5 wild-type and $Ebf2^{-/-}$

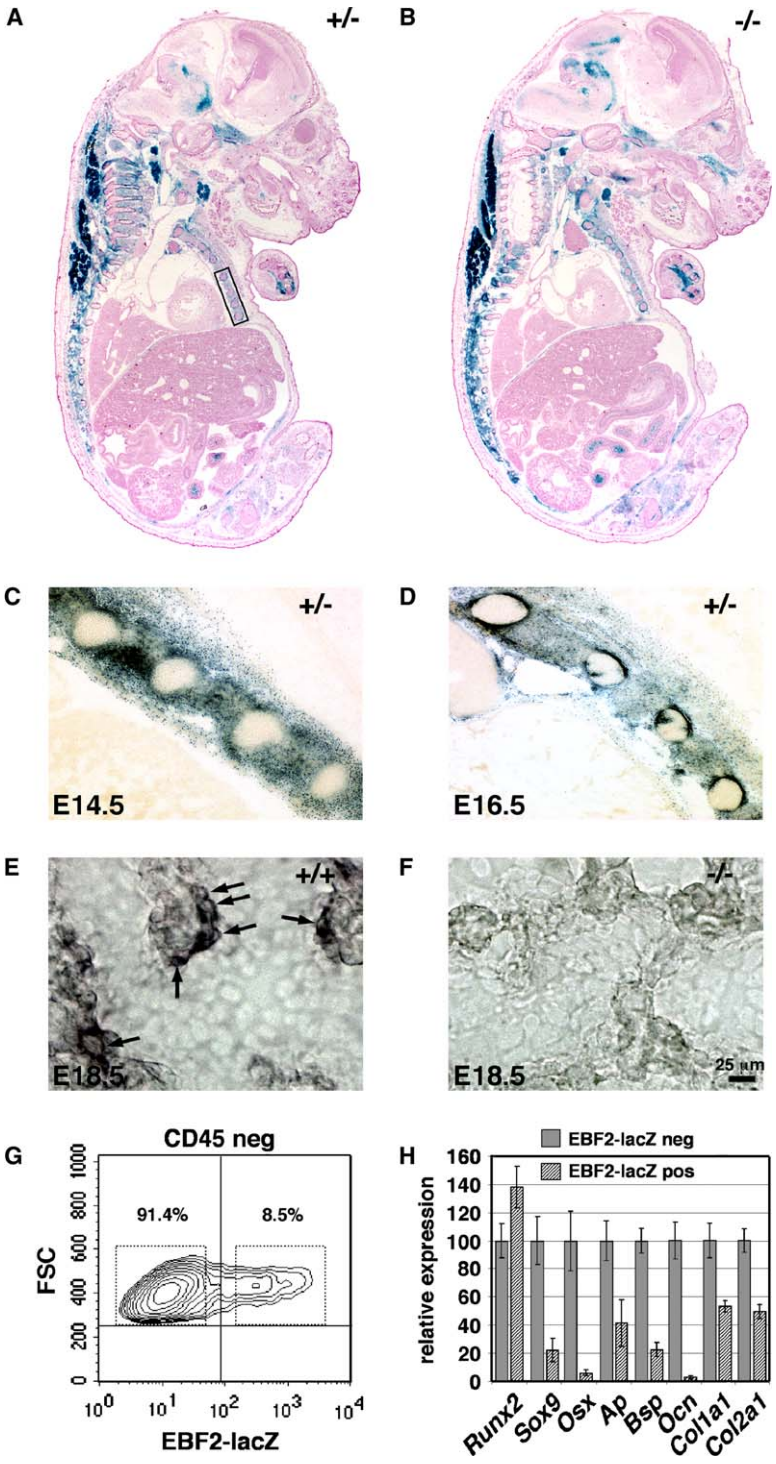

Figure 1. Expression of EBF2 at Sites of Osteogenesis and in a Subset of Osteoblastic Cells

(A and B) Staining for β-galactosidase in cryosections of E16.5 (A) *Ebf2*$^{+/-}$ and (B) *Ebf2*$^{-/-}$ embryos. EBF2-lacZ-positive cells can be detected in adipose tissue and in cells surrounding the cartilaginous structures of future skeletal elements.

(C and D) Magnification of EBF2-lacZ staining in the area surrounding the future ribs (as indicated in (A)) in (C) E14.5 *Ebf2*$^{+/-}$ and (D) E16.5 *Ebf2*$^{+/-}$ embryos.

(E and F) In situ hybridization of the E18.5 tibia to detect *Ebf2* transcripts in (E) *Ebf2*$^{+/+}$ and (F) *Ebf2*$^{-/-}$ embryos. Individual *Ebf2*-expressing cells are attached to cancellous bone in a scattered pattern (arrows).

(G) Cells isolated from bone of neonate *Ebf2*$^{+/-}$ animals are analyzed by flow cytometry to detect EBF2-lacZ-expressing cells. Cells are gated as CD45 negative, and the sorting gates are indicated.

(H) Real-time RT-PCR analysis of the expression of *Runx2*, *Sox9*, *Osterix* (*Osx*), *Alkaline phosphatase* (*Ap*), *Bone sialoprotein* (*Bsp*), *Osteocalcin* (*Ocn*), *Collagen1a1* (*Col1a1*), and *Collagen2a1* (*Col2a1*) in cells from neonatal bones of *Ebf2*$^{+/-}$ mice. The cells were sorted as positive or negative for the expression of EBF2-lacZ as indicated in (G). Error bars represent the standard deviation of the mean of three experiments.

embryos is similar (Figure 2D). However, quantitative RT-PCR assays to detect transcripts encoding regulators of osteoblast differentiation or components of the extracellular matrix indicated that the expression of *bone sialoprotein* and *osteocalcin* is decreased modestly, but reproducibly, in directly sorted *Ebf2*$^{-/-}$ osteoblastic cells, relative to *Ebf2*$^{+/-}$ osteoblasts (Figure 2E). Thus, the lack of EBF2 may result in a small defect in the terminal differentiation of osteoblasts.

To analyze the bones of older mice, we used mice at 3 weeks of age, when the dwarfism and impaired viability of *Ebf2*$^{-/-}$ mice is less severe than in adult mice (Corradi et al., 2003). At 3 weeks of age, the size and weight of the *Ebf2*$^{-/-}$ mice are reduced by 22% and 43%, respectively, relative to wild-type mice. X-ray analysis and histology of the tibia at low resolution showed that tibial length in EBF2-deficient mice is decreased by ~19% relative to wild-type mice (Figures 3A and 3B). Von Kossa

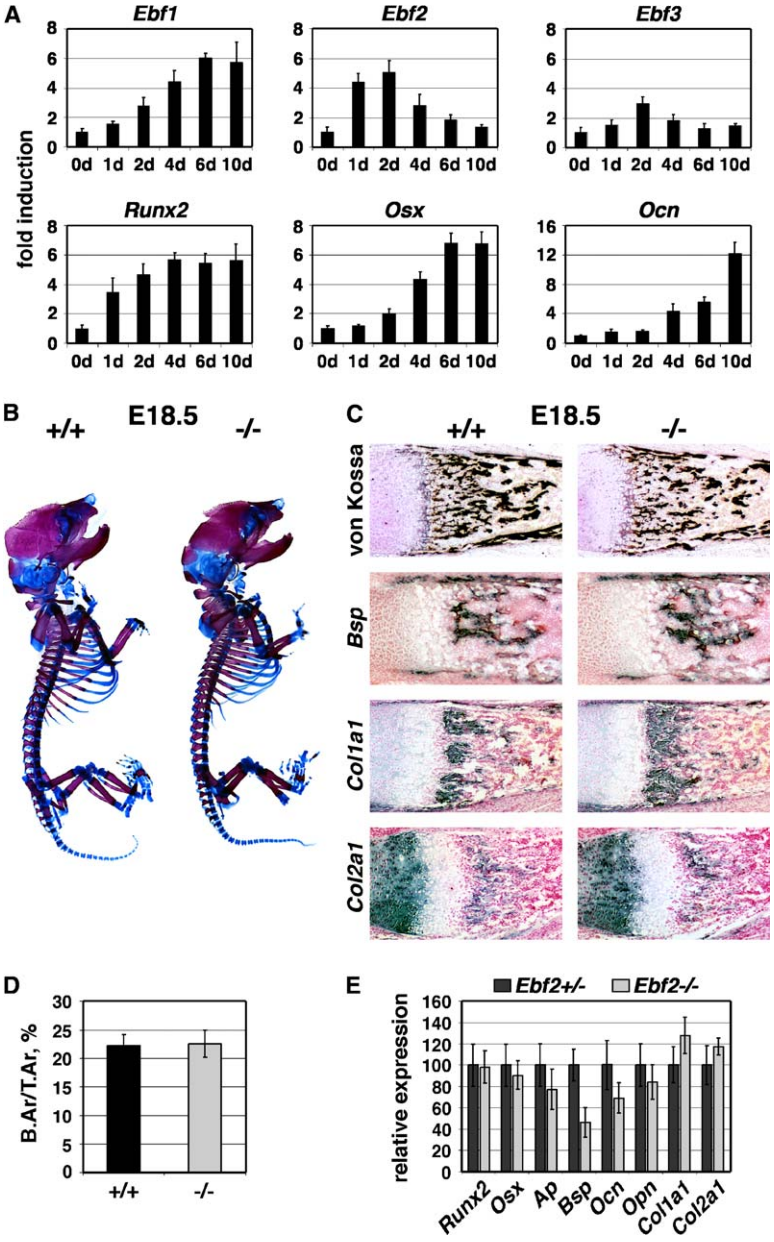

Figure 2. Expression of *Ebf* Genes during Osteoblastic Differentiation and Embryonic Bone Development in the Absence of EBF2

(A) Real-time RT-PCR analysis of the expression of *Ebf1*, *Ebf2*, and *Ebf3* in calvarial cells induced for osteoblastic differentiation for the indicated time points. For comparison, the induction of *Runx2*, *Osterix* (*Osx*), and *Osteocalcin* (*Ocn*) is shown. Error bars represent the standard deviation of the mean of three experiments.

(B) Alcian blue/alizarin red staining of cartilage and bone in the skeleton of E18.5 embryos.

(C) Analysis of sections of E18.5 tibia bone and cartilage by von Kossa staining and in situ hybridizations to detect transcripts of *Bsp*, *Col1a1*, and *Col2a1*.

(D) Histomorphometric analysis of von Kossa-stained femurs of E18.5 embryos. Error bars represent the standard deviation of the mean of four experiments.

(E) Cells isolated from cortical bones of E18.5 $Ebf2^{+/-}$ and $Ebf2^{-/-}$ mice were sorted for the expression of EBF2-lacZ (CD45 negative) and were analyzed for the expression of *Runx2*, *Osx*, *alkaline phosphatase* (*Ap*), *Bsp*, *Ocn*, *Osteopontin* (*Opn*), *Col1a1*, and *Col2a1* by real-time RT-PCR. Error bars represent the standard deviation of the mean of three experiments.

staining of femurs of wild-type and $Ebf2^{-/-}$ mice revealed a cancellous and cortical bone osteopenia in the mutant mice (Figure 3C). The cortical thickness of the femur midshaft, measured by histomorphometry, was reduced by 65% in mutant mice (136 ± 17 μm versus 61 ± 8 μm, wild-type versus $Ebf2^{-/-}$; n = 4–5). High-power micrographs of cortical bone in the midshaft region showed areas of osteoclastic endocortical bone resorption in mutant, but not wild-type, mice (Figure 3C). To quantify the effects of cortical thinning on bone biomechanics, we performed three-point bending tests of femurs from wild-type and $Ebf2^{-/-}$ mice. We found an ~3-fold decrease in ultimate force in $Ebf2^{-/-}$ mice (Figure 3D).

Von Kossa staining also indicated that the cancellous bone area (B.Ar/T.Ar) and the width of the growth plate of $Ebf2^{-/-}$ mice are reduced, whereas the number of adipocytes is increased, as shown for the proximal tibial metaphysis (Figure 3E). Osteoblasts could be detected in normal numbers in histological sections (data not shown), and the rate of cancellous bone formation, as measured by calcein fluorochrome labeling, showed no significant difference between wild-type and $Ebf2^{-/-}$ mice (0.99 ± 0.22 $\mu m^2/\mu m$/day in wild-type versus 1.18 ± 0.18 $\mu m^2/\mu m$/day in $Ebf2^{-/-}$ mice; n = 4–5). Furthermore, quantitative RT-PCR analysis of the expression of osteoblastic marker genes in cells isolated from the tibia of 3-week-old wild-type and EBF2-deficient mice did not reveal any significant differences (Figure S2C). Finally, van Gieson staining of femurs showed a similar density and direction of collagen fibers in $Ebf2^{+/+}$ and $Ebf2^{-/-}$ mice (Figures S2D and S2E). However, we detected an increase in the number of TRAP-positive osteoclasts in EBF2-deficient mice (Figure 3G). Quantification of

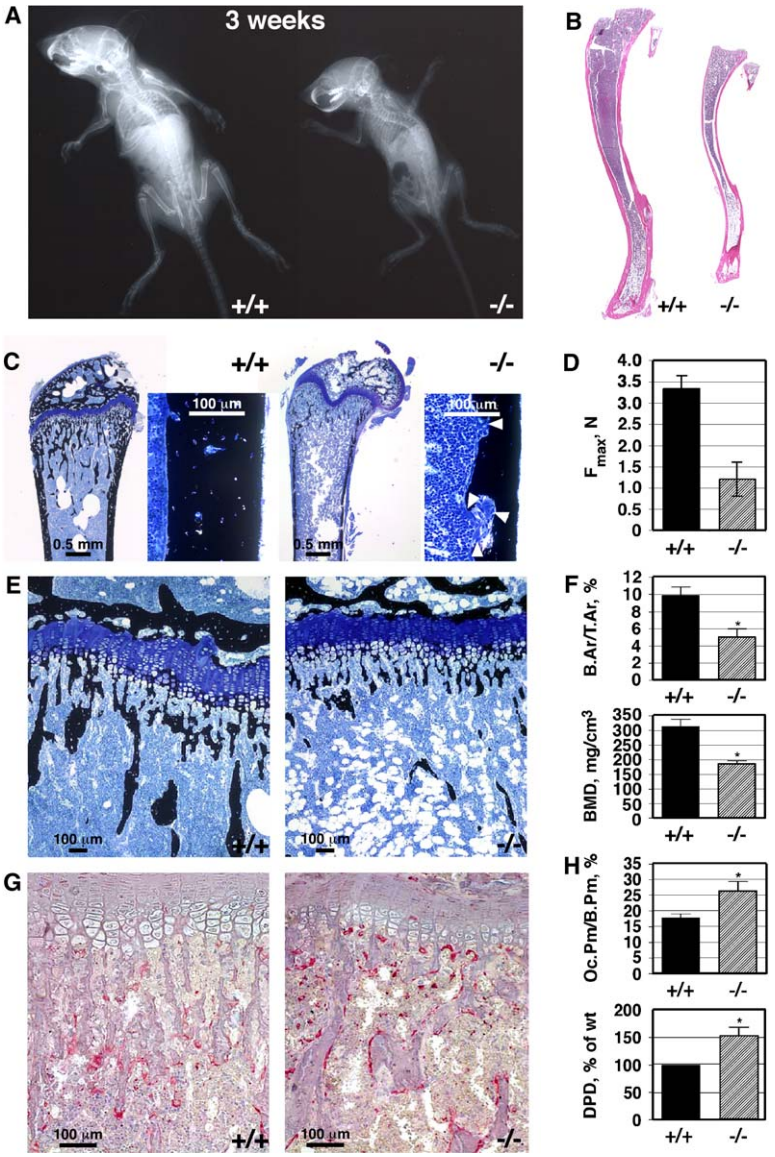

Figure 3. Osteopenia and Increased Osteoclastic Bone Resorption in 3-Week-Old *Ebf2*$^{-/-}$ Mice

(A) X-ray analysis of *Ebf2*$^{+/+}$ (+/+) and *Ebf2*$^{-/-}$ (−/−) mice indicates decreased mineral density in the mutant mice.

(B) Haematoxylin/Eosin staining of the tibia from *Ebf2*$^{+/+}$ and *Ebf2*$^{-/-}$ mice shows a decreased bone length (19%) in the mutant mice.

(C) Von Kossa staining shows reduced bone matrix in femurs of EBF2-deficient mice (left). Higher magnification of the cortical bone area reveals a reduction in thickness by 65% and the presence of osteoclasts (arrowheads) adjacent to cortical bone (right).

(D) Biomechanic testing by three-point bending of femurs; n = 3–4.

(E) Von Kossa staining of sections of the proximal tibia indicates a pronounced cancellous bone osteopenia in the metaphysis of *Ebf2*$^{-/-}$ mice relative to wild-type mice. Mutant mice have a reduction of cortical bone thickness, and they show an increase in the number of bone marrow fat cells (white).

(F) Bone histomorphometry reveals a 49% reduction in the tibial cancellous bone area (B.Ar/T.Ar., %) in *Ebf2*$^{-/-}$ mice (top). Peripheral quantitative computed tomography (pQCT) shows a decrease in the total bone mineral density (BMD, mg/cm^3) of the distal femoral metaphysis by 40% in *Ebf2*$^{-/-}$ mice (bottom). n = 4–5.

(G) Staining to detect tartrate-resistant acid phosphatase (TRAP)-positive osteoclasts indicates that *Ebf2*$^{-/-}$ mice have an increased number of differentiated osteoclasts (stained in red) covering the bone surface.

(H) Osteoclast perimeter (Oc.Pm/B.Pm, %) is increased by 47% in *Ebf2*$^{-/-}$ mice relative to wild-type mice (top). Urinary excretion of the bone resorption marker deoxypyridinoline (DPD) is elevated in *Ebf2*$^{-/-}$ mice (bottom). DPD excretion is corrected for creatinine excretion, and it is expressed as a percentage of wild-type control. n = 4–5.

*p < 0.05 as compared with wild-type by t test. Error bars in (D), (F), and (H) represent the standard deviation of the mean of the analysis of four to five mice.

these defects by bone histomorphometry indicated that the trabecular bone area of the tibia is reduced by 49% relative to wild-type mice (Figure 3F). These findings were confirmed by peripheral quantitative computer tomography (pQCT), showing that the bone mineral density (BMD) of both the distal metaphysis and shaft of the femur of *Ebf2*$^{-/-}$ mice is diminished by 40% (Figure 3F; Table S1). Finally, the osteoclast perimeter (Oc.Pm/B.Pm), a measurement of the surface of bone covered by osteoclasts, was increased by 47%, and the urinary excretion of the collagen degradation product deoxypyridinoline (DPD), a whole body marker for bone resorption, was elevated by 50% in the mutant mice (Figure 3H). Taken together, these data indicate that the osteopenia in EBF2-deficient mice, which is more pronounced than can be accounted for by the dwarfism, is due to an increased bone resorption and enhanced osteoclastogenesis.

Deregulated Expression of *Osteoprotegerin* and *Rankl* in *Ebf2*$^{-/-}$ Osteoblasts

The observed increase in the number of osteoclasts in EBF2-deficient mice prompted us to examine the expression of components of the RANK-RANKL signaling pathway that regulate communication between osteoblasts and osteoclasts. In a first step, we examined the expression of the *Rankl* and *Opg* genes by immunohistochemistry on tibia bones from *Ebf2*$^{+/+}$ and *Ebf2*$^{-/-}$ E18.5 embryos (Figures 4A and 4B). Expression of OPG and RANKL proteins could be detected in cells adjacent to trabecular bone. Relative to wild-type mice, however, the expression of OPG appeared weaker, and that of RANKL appeared stronger, in *Ebf2*$^{-/-}$ mice. To confirm the putative changes in the expression of these components of the RANK-RANKL signaling pathway, we purified osteoblasts from the calvariae of heterozygous and homozygous mutant newborn mice by sorting for

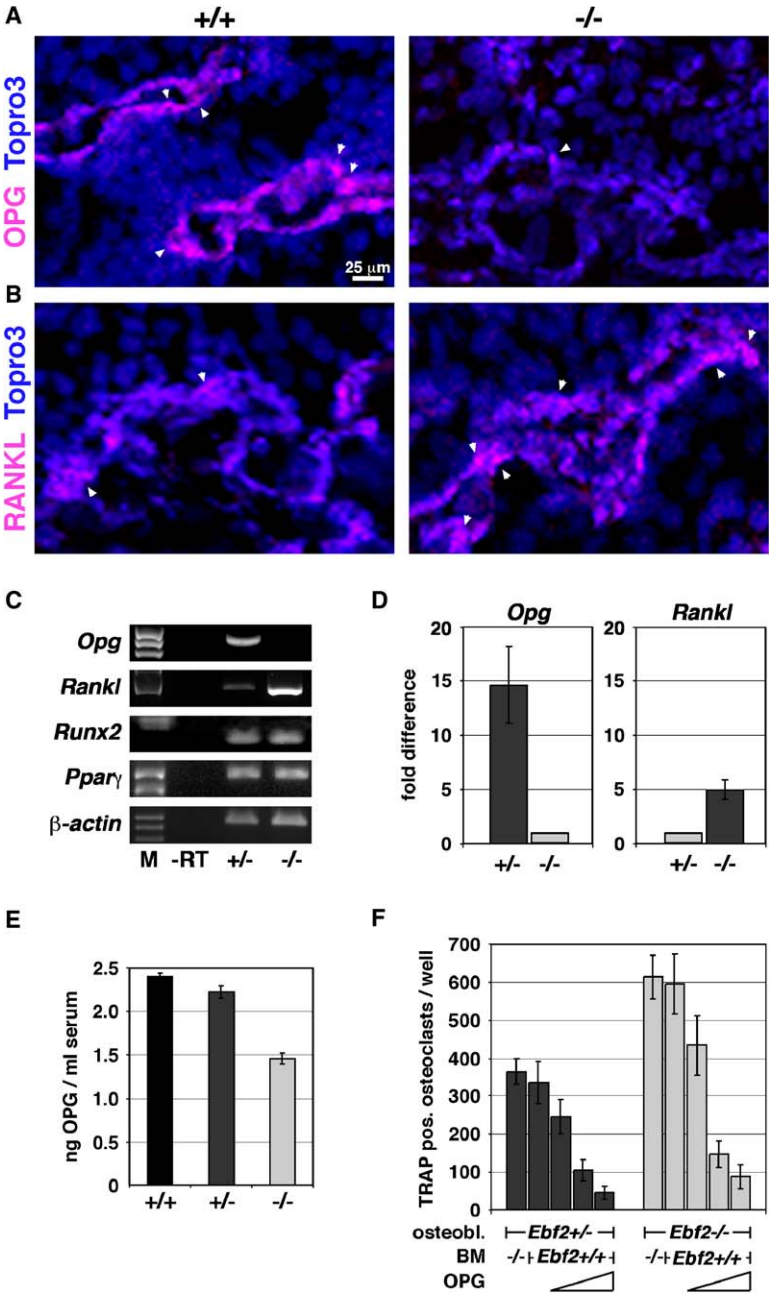

Figure 4. Deregulated Expression of Osteoprotegerin and Rankl in *Ebf2*$^{-/-}$ Osteoblasts and Osteoblast-Dependent Bone Resorption Defect

(A and B) Immunohistochemical staining for (A) Osteoprotegerin (OPG) and (B) RANKL in sections of tibias of *Ebf2*$^{+/+}$ and *Ebf2*$^{-/-}$ mice. Topro3 was used for the staining of DNA.

(C) RT-PCR analysis to detect transcripts of *Opg*, *Rankl*, *Runx2*, and *Pparγ* in *Ebf2*$^{+/-}$ and *Ebf2*$^{-/-}$ calvarial cells that have been isolated under standard conditions for osteoblasts, expanded in culture (two passages), and sorted for the expression of EBF2-lacZ.

(D) Real-time RT-PCR analysis of *Opg* and *Rankl* mRNA in sorted osteoblasts without prior in vitro culture. Error bars represent the standard deviation of the mean of three experiments.

(E) Determination of serum levels of OPG from *Ebf2*$^{+/+}$, *Ebf2*$^{+/-}$, and *Ebf2*$^{-/-}$ mice by ELISA reveals a reduction of OPG in the absence of EBF2 by 40%. Error bars represent the standard deviation of the mean of four experiments.

(F) Enhanced osteoclast differentiation on *Ebf2*$^{-/-}$ osteoblasts in vitro is reversed by recombinant OPG. EBF2-lacZ-positive osteoblastic cells from *Ebf2*$^{+/-}$ and *Ebf2*$^{-/-}$ mice were sorted by flow cytometry and were cocultured with primed bone marrow cells (BMs) from *Ebf2*$^{+/+}$ or *Ebf2*$^{-/-}$ mice as indicated. Recombinant OPG protein was added at three different concentrations (5, 25, and 50 ng/ml) into the osteoblast-BM coculture, and the appearance of TRAP-positive cells was measured after 5 days of coculture. Error bars represent the standard deviation of the mean of three experiments.

β-galactosidase activity, expanded the cells in culture, and analyzed the expression of putative EBF2 target genes by RT-PCR. In EBF2-deficient osteoblasts, the number of *Opg* transcripts was markedly reduced, whereas the number of *Rankl* transcripts was increased (Figure 4C). No significant changes in the expression of *Runx2* and *Pparγ* were observed (Figure 4C). With the aim of quantifying these effects and extending the observations to cells that have not been cultured in vitro, we performed quantitative RT-PCR to detect transcripts in heterozygous and homozygous EBF2-expressing osteoblastic cells that have been sorted directly after isolation. In homozygous mutant cells, the expression of *Opg* was decreased by a factor of 14, and the expression of *Rankl* was increased by a factor of 5 (Figure 4D).

Osteoblast-Autonomous Defect of Osteoclast Differentiation in *Ebf2*$^{-/-}$ Mice

The increase in osteoclast numbers in the bones of EBF2-deficient mice and the downregulation of *Opg* expression in *Ebf2*$^{-/-}$ osteoblasts raised questions as to whether these defects result in a decrease in the serum levels of OPG and whether the defects are osteoblast autonomous. Although OPG is expressed by a variety of cell types, the levels of OPG in the serum of 3-week-old *Ebf2*$^{-/-}$ mice were reduced by 41% relative to wild-type mice (Figure 4E). We also examined whether the defects in osteoclastogenesis can be recapitulated in vitro and overcome by the addition of recombinant OPG. Toward this end, we incubated wild-type bone marrow cells with macrophage colony-stimulating factor (M-CSF) to

enrich for osteoclast precursors, and we cultured these cells on osteoblastic cells from heterozygous and homozygous mutant mice that had been sorted for the expression of EBF2-lacZ. Osteoblast-mediated differentiation of the bone marrow cells into osteoclasts was monitored by TRAP staining. The number of osteoclasts in the coculture with *Ebf2*$^{-/-}$ osteoblasts was 57% higher than in the coculture with *Ebf2*$^{+/-}$ osteoblasts (Figure 4F). As a control, no difference in the generation of osteoclasts was observed with EBF2-deficient bone marrow cells compared to wild-type bone marrow cells. If the increase in the differentiation of osteoclasts is dependent on the decrease of OPG expression in *Ebf2*$^{-/-}$ osteoblasts, it should be possible to reverse the defect by the addition of exogenous OPG protein. Therefore, we added increasing amounts of recombinant OPG to the bone marrow cells being cultured with *Ebf2*$^{+/-}$ or *Ebf2*$^{-/-}$ osteoblasts. In both cocultures, the numbers of TRAP-positive osteoclasts were reduced in a dose-dependent manner, although more exogenous OPG is needed in the *Ebf2*$^{-/-}$ cultures to achieve a similar block in osteoclast differentiation as in the *Ebf2*$^{+/-}$ cultures. Therefore, the enhanced differentiation of osteoclasts on EBF2-deficient osteoblasts appears to be linked to the decrease in the expression of OPG. Moreover, these data indicate that the osteoclast defect in *Ebf2*$^{-/-}$ mice is osteoblast autonomous.

Osteoprotegerin Is a Direct Target for EBF2

To examine whether *Opg* or *Rankl* are direct or indirect targets of EBF2, we searched for binding sites of EBF proteins in the promoter of these genes. No binding sites could be identified in the murine *Rankl* promoter (Kitazawa et al., 1999). In the promoter of the human *OPG* gene, which has been functionally characterized (Thirunavukkarasu et al., 2000), four potential EBF binding sites were identified in a region 1.5 kb upstream of the transcription start site. Two of these sites at −993 and −184 were confirmed as bona fide binding sites in an electrophoretic mobility shift assay (Figures 5A and 5B). For this experiment, we used the DNA binding and dimerization domain of EBF1, which can be purified in recombinant and soluble form and has the same DNA binding specificity as EBF2 (Hagman et al., 1993; Malgaretti et al., 1997). The efficiency of binding to the −184 site of the *OPG* promoter was similar to that of the high-affinity site in the *mb1* promoter (Travis et al., 1993). The specificity of DNA binding was confirmed by the lack of EBF binding to a mutant (mut) site. Binding of EBF to the second site at −993 of *OPG* was observed at an ~3-fold lower efficiency (Figure 5B). We also confirmed the binding of EBF2 to the site at −184 by using nuclear extracts from 293 cells that express EBF2, but not EBF1 (data not shown), and by competing with specific or nonspecific oligonucleotides (Figure S2F).

Previous analysis of the *OPG* promoter indicated that truncations between 5.9 kb and 0.4 kb have modest effects on the basal promoter activity and on the responsiveness of the promoter to TGFβ signals (Thirunavukkarasu et al., 2001). Therefore, we examined the functional importance of EBF2 in the context of a 700 bp promoter fragment containing the wild-type or a mutated EBF binding site at −184. Transient transfection of *OPG-luciferase* gene constructs (*OPG-luc*) into HeLa cells, alone or together with an expression plasmid for EBF2, indicated that EBF2 augments the activity of the wild-type *OPG* promoter fragment by a factor of six, whereas the point-mutated promoter was stimulated only 2-fold (Figure 5C). Based on the presence of a Runx2 binding site at −303 (Thirunavukkarasu et al., 2000), we also cotransfected the *OPG-luc* reporter construct with a Runx2 expression plasmid. No significant activation was observed, consistent with the lack of an effect of mutation of the Runx2 binding site in an osteosarcoma cell line (Thirunavukkarasu et al., 2001). However, Runx2 could potentiate the EBF2-mediated activation of the *OPG-luc* reporter by a factor of two, suggesting that these transcription factors may modestly cooperate in the regulation *OPG* (Figure 5C). Moreover, transfection of the wild-type and mutated *OPG-luc* reporters into C2C12 cells, which express low levels of EBF2, indicate that the mutation of the EBF2 binding site decreases reporter gene expression by a factor of two (Figure 5D; data not shown).

Recently, the *OPG* gene was shown to be directly regulated by LEF1 and β-catenin in response to Wnt signaling (Glass et al., 2005). Therefore, we examined whether EBF2 cooperates with the Wnt signaling pathway in the regulation of *OPG*. Toward this end, we transfected HeLa cells with the *OPG-luc* reporter, together with the expression plasmid for EBF2 alone, or in combination with LEF1 and β-catenin (Figure 5E). The activity of the *OPG* promoter was augmented modestly by either EBF2 or LEF1/β-catenin alone, but it was markedly increased by the combination of EBF2 and LEF1/β-catenin.

To further examine the role of EBF2, Runx2, and LEF1/β-catenin in the regulation of the endogenous *OPG* gene, we transfected the EBF2 or Runx2 expression plasmids, alone or in combination, into HeLa cells and analyzed the expression of *OPG* by quantitative RT-PCR. Both EBF2 and LEF1/β-catenin could induce the expression of endogenous *OPG*, but the activation was more efficient in cells that have been transfected with both EBF2 and LEF1/β-catenin expression plasmids (Figure 5F). Taken together, these data indicate that EBF2 directly regulates the expression of *OPG* and synergizes strongly with components of the Wnt signaling pathway.

Discussion

Our study identifies EBF2 as a regulator of osteoclastogenesis and bone homeostasis that acts upstream of RANKL signaling. The role of EBF2 in the regulation of *OPG* is based on multiple lines of evidence. First, the expression of *Opg* in sorted EBF2-deficient osteoblastic cells is reduced 14-fold. Moreover, the expression of EBF2 in HeLa cells activates the *OPG* promoter via binding to specific sites in the promoter region, and EBF2 induces the expression of the endogenous *OPG* gene. *Opg* is not only expressed in osteoblastic cells, but it is also expressed in several other cell types, including cells that are negative for the expression of EBF2 (Simonet et al., 1997). Therefore, it is likely that other transcription factors also participate in the regulation of the expression of OPG. Runx2, a key regulator of the osteoblast cell lineage, has been shown to regulate the promoter of *OPG* in transient transfection experiments (Thirunavukkarasu et al., 2000). However, *Opg* is efficiently

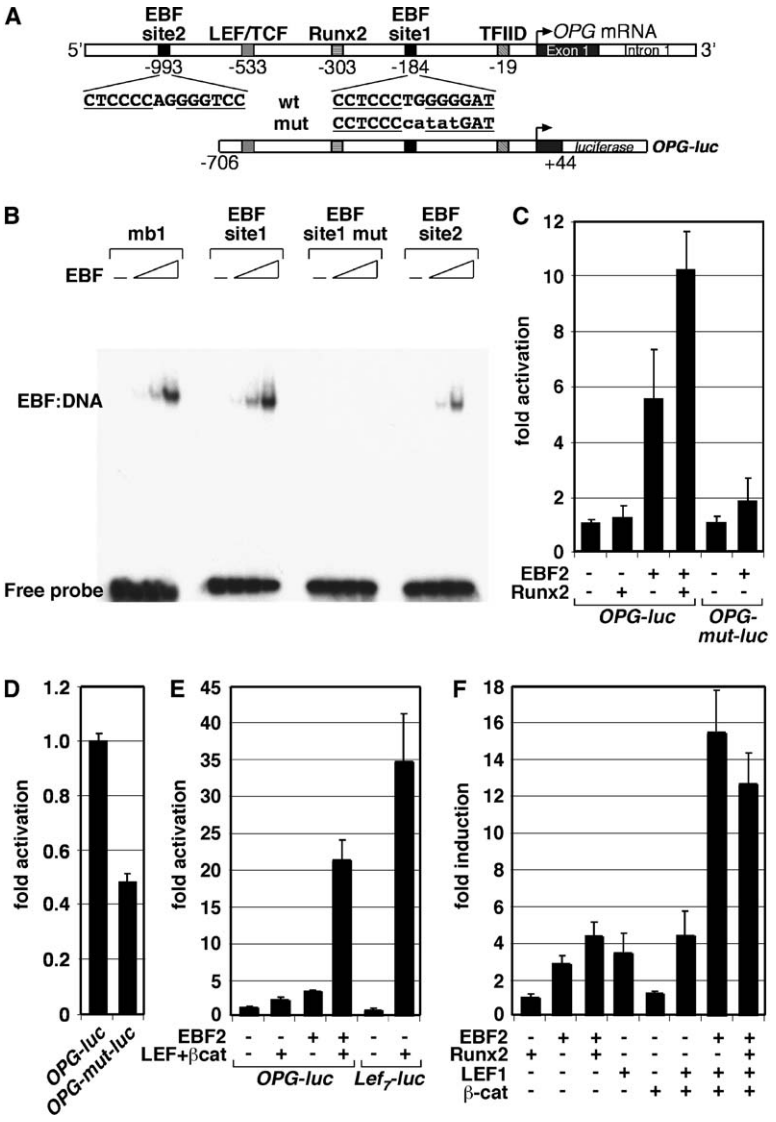

Figure 5. Direct Regulation of *Opg* by EBF2

(A) Schematic representation of binding sites for EBF, LEF/TCF, and Runx2 proteins in the human *OPG* promoter. Sequences and positions of wild-type (wt) and mutated (mut) EBF binding sites relative to the transcriptional start site are indicated. The mutations are shown in lower case letters.

(B) Electrophoretic mobility shift assay (EMSA) to detect binding of the recombinant DNA binding and dimerization domain of EBF1 (30, 100, and 300 ng) to ^{32}P-labeled oligonucleotides encompassing the EBF binding sites in the *OPG* or *mb1* promoters (Travis et al., 1993).

(C) HeLa cells were transiently transfected with 0.3 μg luciferase reporter (*OPG-luc*) alone, or together with 0.8 μg expression plasmids for EBF2 or 0.8 μg Runx2, as indicated. The same mutation as in the EMSA (see [A] and [B]) was used in the luciferase construct as a control (*OPG-mut-luc*). The levels of luciferase activity were normalized to the expression of a cytomegalovirus β-galactosidase reporter plasmid. In all reporter assays, the values represent duplicates of representative transfections.

(D) C2C12 cells, which express *Ebf2*, were transfected with the *OPG-luc* or *OPG-mut-luc* reporter plasmids as described above.

(E) HeLa cells were transiently transfected with 0.1 μg *OPG-luc* reporter alone, or together with expression plasmids for EBF2 (0.4 μg) or LEF-1 (50 ng) and β-catenin (0.5 μg), as indicated. As a positive control, a *Lef$_7$-luciferase* reporter, containing multimerized LEF1 binding sites, was used. The levels of luciferase activity were normalized for β-galactosidase activity. In the reporter assays (C–E), error bars represent the deviation from the mean of duplicate transfections.

(F) HeLa cells were transiently transfected with expression plasmids for Runx2, EBF2, LEF1, or β-catenin alone, or in combination, as indicated. The expression of the endogenous *OPG* gene was measured by real-time PCR. Since *OPG* transcripts could not be detected in mock-transfected cells, the lowest value (Runx2 transfection) was set to 1. Error bars represent the standard deviation of the mean of three experiments.

expressed in a *Runx2*$^{-/-}$ calvaria-derived cell line, and forced expression of Runx2 via adenoviral transduction of these cell results in suppression of *Opg* and activation of *Rankl* expression (Enomoto et al., 2003). In addition, it has been shown that Runx2 is not essential for vitamin D-regulated expression of *Rankl* and *Opg* in osteoblastic cells (Notoya et al., 2004). Moreover, our transfection experiments in HeLa cells indicate that Runx2 has only a modest effect on the activity of the *OPG* promoter construct, although Runx2 could augment the expression of the endogenous *OPG* gene. Thus, the effects of Runx2 on the expression of *OPG* are likely to be indirect.

Another member of the Runx family of transcription factors, Runx1, has been shown to cooperate with EBF1 in the lymphocyte-specific regulation of the *mb1* gene (Maier et al., 2004). In this context, EBF1 and Runx1 bind to adjacent binding sites in the *mb1* promoter and mediate DNA hypomethylation and changes in chromatin structure. Therefore, either or both of these proteins appear to act as "pioneer factors" in the transcriptional activation of target genes.

Recently, Karsenty and coworkers have found that the Wnt signaling pathway regulates osteoblast expression of *Opg* (Glass et al., 2005). Induced stabilization of β-catenin in osteoblasts was found to result in a higher bone mass, whereas conditional deletion of β-catenin resulted in osteopenia. Moreover, expression of *Opg* was found to be upregulated in osteoblasts containing stabilized β-catenin and downregulated in osteoblasts from which β-catenin has been deleted (Glass et al., 2005). This study also showed that the Wnt-responsive transcription factor TCF1 binds directly to three sites in a 3.6 kb promoter fragment of the *Opg* gene in vitro and in vivo. Consistent with our observations, no binding of Runx2 to the *Opg* promoter was detected in chromatin immunoprecipitation experiments in vivo (Glass et al., 2005). In contrast to the weak cooperation of EBF2 and Runx2 in the regulation of the *Opg* gene, we found

a strong synergy between EBF2 and LEF1, a member of the LEF1/TCF family of Wnt-responsive transcription factors. Both EBF2 and LEF1/TCF proteins are expressed in specific cell types, and the functional synergy may contribute to a more restricted pattern of Wnt-regulated expression of *Opg*.

In addition to the effects of Wnt signaling in differentiated osteoblasts that includes the regulation of *Opg*, β-catenin also has an effect in osteoblast precursors, because the conditional deletion of β-catenin in mesenchymal progenitor cells prevents differentiation into osteoblasts (Hill et al., 2005). Therefore, the functional synergy between EBF2 and LEF1 may operate only at specific target genes that include *Opg*.

EBF2 may also be involved in multiple aspects of osteoblast function and/or differentiation. Although EBF2 regulates the expression of *Opg* in osteoblastic cells, the targeted gene inactivation of *Ebf2* has no major effect on the generation of osteoblasts or on the rate of bone formation, suggesting that EBF2 is dispensable for osteoblast differentiation and function. However, EBF2 may act in a redundant manner with other members of the EBF family of transcription factors in regulating osteoblast differentiation. Consistent with this possibility, EBF1 and EBF3 transcripts can be detected in EBF2-expressing osteoblastic cells. Interestingly, the temporal patterns of the expression of specific members of the EBF family of transcription factors differ during osteoblast differentiation. In an in vitro model for osteoblast differentiation (Bellows et al., 1990), abundant expression of *Ebf2* is already detected at 2 days of culture, but ceases after 1 week of culture. In contrast, the expression of *Ebf1*, together with *Osterix*, peaks after 1 week of culture. The combined inactivation of both *Ebf1* and *Ebf2* should shed light on the potential redundancy of EBF proteins in osteoblast differentiation.

To date, our insight into the regulation of the activity of EBF proteins is still limited. The DNA binding ability of EBF1 has been found to be inhibited by Notch signaling (Smith et al., 2005), raising the possibility that a similar regulation may modulate the activity of EBF2. Thus, multiple signaling pathways may regulate the differentiation of osteoclasts via osteoblast-specific transcription factors that act on promoters of genes involved in RANK-RANKL signaling. In addition, signaling by interferon-β, which is activated by *c-fos*, antagonizes the RANK-mediated regulation of *c-fos* in osteoclasts, generating a regulatory feedback loop (Takayanagi et al., 2002b). An insight into the regulatory network of transcription factors that regulates RANK-RANKL signaling will be important for the detailed understanding of the homeostatic interactions between osteoblasts and osteoclasts.

Experimental Procedures

PCR, RT-PCR, and Real-Time PCR

Genotyping of *Ebf2* mutant animals was performed as described (Corradi et al., 2003). RT-PCR was carried out according to standard protocols, by using Superscript II reverse transcriptase (Invitrogen) and the oligo-dT primer (Roche). Real-time PCR was performed with SYBR GREEN PCR master mix (Applied Biosystems) and the ABI PRISM 7000 sequence detection system (Applied Biosystems). The sequences for primer pairs used in PCR reactions are given in Supplemental Experimental Procedures. Three independent measurements were performed for each PCR analysis.

Isolation and Cultivation of Cells

Preparation of osteoblastic cells from neonate bones was performed as described (Bakker and Klein-Nulend, 2003). Hindlegs from animals of the respective genotypes were isolated, and muscle and other tissue were removed. The bones were cleaned quickly in alcohol and PBS and were shaken for 15 min at 37°C in αMEM medium containing 0.1% collagenase (Sigma) and 0.2% neutral dispase II (Roche). This was repeated once, and the first two fractions were discarded. Subsequently, bones were incubated in the described medium three more times. These fractions were collected, and cells isolated from the fractions were immediately subjected to FDG loading and FACS analysis. Osteoblasts were also isolated from calvariae of day 2–5 newborn animals, and osteoblast-osteoclast coculture experiments were performed as described (Jochum et al., 2000). A total of 10^5 osteoblasts/well (24-well plate) were sorted as lacZ$^+$ from *Ebf2*$^{+/-}$ and *Ebf2*$^{-/-}$ mice and were allowed to attach to the plastic dish overnight. Osteoblasts were incubated with 10^6 bone marrow cells per well. These bone marrow cells had been primed as osteoclast progenitors by overnight incubation with 5 ng/ml M-CSF. The incubation medium for coculture was αMEM, supplemented with 10% FCS, 10^{-8} M 1α,25$(OH)_2D_3$-dihydroxyvitamin D3, and 10^{-7} M dexamethasone. Osteoclast differentiation was measured by TRAP staining after 5 days. Chondrocytes used in real-time PCR were sorted cells from Col2-GFP transgenic mice (kind gift from Christine Hartmann; Grant et al., 2000). In vitro differentiation of osteoblasts was carried out by culturing freshly isolated calvarial cells in αMEM medium as described above. After 3 days, osteoblastic differentiation was induced by adding 100 mM β-glycerophosphate and 50 ng/ml ascorbic acid to the medium.

β-Galactosidase Detection and Flow Cytometry

For sorting of EBF2-lacZ-positive cells, osteoblastic cells were loaded with fluorescein digalactoside (FDG; Molecular Probes) through hypotonic shock (75 s at 37°C) as described by the manufacturer. For each sample, propidium iodide (Sigma) was used to gate out dead cells.

In Situ Hybridization and Immunohistochemistry

In situ hybridization was performed as described (Malgaretti et al., 1997). The riboprobe for *Ebf2* was generated from the full-length cDNA (Malgaretti et al., 1997). For immunohistochemistry, comparable sections were fixed in 4% PFA for 15 min, washed in TBST 0.1% Triton X-100, blocked for 2 hr at room temperature in 10% goat serum, and incubated with primary antibody overnight at 4°C. As first antibody, either biotinylated anti-mouse OPG (R&D Systems, BAF459) or biotinylated anti-mouse RANKL (R&D Systems, BAF462) was used at a concentration of 1:20. After washing, streptavidin-AlexaFluor546 conjugate was used to detect primary antibody (2 mg/ml; 1:500). For nuclear staining, specimens were treated with TOPRO3 (Molecular Probes).

Bone Histology and Histomorphometry

Processing of bone specimens and cancellous bone histomorphometry in the proximal tibial metaphysis were performed as described (Erben, 1997). The area within 0.25 mm from the growth plate was excluded from the measurements in 3-week-old mice. In distal femurs from E18.5 embryos, the cancellous bone, including calcified cartilage, from the growth cartilage-metaphyseal junction until mid-diaphysis was measured in von Kossa-stained paraffin sections.

Bone Mineral Density Measurements and Radiography

Bone mineral density (BMD) of the left femur was measured by peripheral quantitative computed tomography (pQCT) by using a XCT Research M+ pQCT machine (Stratec Medizintechnik). One slice (0.2 mm thick) in the mid-diaphysis of the femur and three slices in the distal femoral metaphysis located 1.5, 2, and 2.5 mm proximal to the articular surface of the knee joint were measured. BMD values of the distal femoral metaphysis were calculated as the mean over three slices. A voxel size of 0.070 mm and a threshold of 600 mg/cm^3 were used for calculation of cortical BMD.

Bone Biomechanics

Femur bones were prepared from 3-week-old mice and were loaded to failure by three-point bending tests, by using a Zwick Z020/TN2A

materials testing machine with a force resolution of 0.1 N. The distance between the lower supports was 5 mm, and the crosshead speed during testing was 0.2 mm/s. From the force-displacement data, ultimate force (Fmax, N) was calculated.

ELISA

Serum from 3-week-old sex-matched animals (n = 4) was isolated, and OPG levels were measured by using the Quantikine mouse OPG ELISA kit (R&D systems).

EMSA

EBF protein (Hagman et al., 1993) was generated as a HIS tag fusion protein in *E. coli*, and purification was performed by using the HIS tag according to standard procedures. A total of 30, 100, or 300 ng purified EBF, or 3 or 10 μg nuclear extract from 293T cells, were mixed with 10,000 cpm ^{32}P-labeled probe and 100 ng/μl dI/dC in a 20 μl reaction mix as previously described (Hagman et al., 1993). For a list of oligonucleotides, see Supplemental Experimental Procedures. Reactions were incubated at 20ºC for 30 min and then run on a 6% nondenaturating acrylamide gel.

Gene Constructs, Transfection, and Luciferase Assay

The 1.3 kb fragment of the *OPG* promoter (*OPG-luc*) was cloned by PCR amplification from genomic DNA (for primers, see Supplemental Experimental Procedures) and were subcloned into pGL3-basic (Promega). The truncation of the *OPG* promoter (*OPG-luc*; −706 to +44) was carried out by cutting *OPG-luc* with NheI and ApaI and religation. The mutation of EBF binding site f1 was performed by site-directed mutagenesis (for primers, see Supplemental Experimental Procedures). HeLa cells were transfected with 2 μg plasmid DNA and 10 μg salmon sperm DNA by the calcium phosphate method. Cells were harvested 36–48 hr posttransfection in 100 μl reporter lysis buffer. Luciferase assays were conducted according to the manufacturer's instructions (Promega), and β-galactosidase assays were performed as described (Starr et al., 1996).

Supplemental Data

Supplemental Data including the embryonic expression pattern of EBF2, peripheral quantitative computed tomography (pQCT) of 3-week-old mice, and further characterization of EBF2 function are available at http://www.developmentalcell.com/cgi/content/full/9/6/757/DC1/.

Acknowledgments

We thank Drs. Erwin Wagner, Gerard Karsenty, Reinhard Fässler, and Christine Hartman for helpful discussions and critical reading of the manuscript. We are grateful to Bianka Ksienzyk, Christian Buske, and Michaela Feuring-Buske for FACS sorting; Christine Hartmann and Javad Naseri for help with in situ hybridizations; and Jean-Pierre David and Latifah Bakiri for advice with osteoblast cultures and osteoblast-osteoclast cocultures. Furthermore, we would like to thank Wera Roth for her help with the Ebf2 mouse colony. This work was supported by a grant from the Bavarian research foundation (Forimmun, T1) and funds of the Max-Planck Society. The *Ebf2* null mouse was produced thanks to a grant by the Italian Telethon to G.G.C.

Received: June 15, 2005
Revised: September 20, 2005
Accepted: October 17, 2005
Published: December 5, 2005

References

Bakker, A., and Klein-Nulend, J. (2003). Osteoblast isolation from murine calvariae and long bones. Methods Mol. Med. *80*, 19–28.

Baron, R. (2004). Arming the osteoclast. Nat. Med. *10*, 458–460.

Bellows, C.G., Heersche, J.N., and Aubin, J.E. (1990). Determination of the capacity for proliferation and differentiation of osteoprogenitor cells in the presence and absence of dexamethasone. Dev. Biol. *140*, 132–138.

Bucay, N., Sarosi, I., Dunstan, C.R., Morony, S., Tarpley, J., Capparelli, C., Scully, S., Tan, H.L., Xu, W., Lacey, D.L., et al. (1998). Osteoprotegerin-deficient mice develop early onset osteoporosis and arterial calcification. Genes Dev. *12*, 1260–1268.

Corradi, A., Croci, L., Broccoli, V., Zecchini, S., Previtali, S., Wurst, W., Amadio, S., Maggi, R., Quattrini, A., and Consalez, G.G. (2003). Hypogonadotropic hypogonadism and peripheral neuropathy in Ebf2-null mice. Development *130*, 401–410.

de Crombrugghe, B., Lefebvre, V., and Nakashima, K. (2001). Regulatory mechanisms in the pathways of cartilage and bone formation. Curr. Opin. Cell Biol. *13*, 721–727.

Dougall, W.C., Glaccum, M., Charrier, K., Rohrbach, K., Brasel, K., De Smedt, T., Daro, E., Smith, J., Tometsko, M.E., Maliszewski, C.R., et al. (1999). RANK is essential for osteoclast and lymph node development. Genes Dev. *13*, 2412–2424.

Dubois, L., and Vincent, A. (2001). The COE—Collier/Olf1/EBF—transcription factors: structural conservation and diversity of developmental functions. Mech. Dev. *108*, 3–12.

Ducy, P., Zhang, R., Geoffroy, V., Ridall, A.L., and Karsenty, G. (1997). Osf2/Cbfa1: a transcriptional activator of osteoblast differentiation. Cell *89*, 747–754.

Eames, B.F., Sharpe, P.T., and Helms, J.A. (2004). Hierarchy revealed in the specification of three skeletal fates by Sox9 and Runx2. Dev. Biol. *274*, 188–200.

Enomoto, H., Shiojiri, S., Hoshi, K., Furuichi, T., Fukuyama, R., Yoshida, C.A., Kanatani, N., Nakamura, R., Mizuno, A., Zanma, A., et al. (2003). Induction of osteoclast differentiation by Runx2 through receptor activator of nuclear factor-κ B ligand (RANKL) and osteoprotegerin regulation and partial rescue of osteoclastogenesis in Runx2−/− mice by RANKL transgene. J. Biol. Chem. *278*, 23971–23977.

Erben, R.G. (1997). Embedding of bone samples in methylmethacrylate: an improved method suitable for bone histomorphometry, histochemistry, and immunohistochemistry. J. Histochem. Cytochem. *45*, 307–313.

Garel, S., Marin, F., Mattei, M.G., Vesque, C., Vincent, A., and Charnay, P. (1997). Family of Ebf/Olf-1-related genes potentially involved in neuronal differentiation and regional specification in the central nervous system. Dev. Dyn. *210*, 191–205.

Glass, D.A., 2nd, Bialek, P., Ahn, J.D., Starbuck, M., Patel, M.S., Clevers, H., Taketo, M.M., Long, F., McMahon, A.P., Lang, R.A., and Karsenty, G. (2005). Canonical Wnt signaling in differentiated osteoblasts controls osteoclast differentiation. Dev. Cell *8*, 751–764.

Grant, T.D., Cho, J., Ariail, K.S., Weksler, N.B., Smith, R.W., and Horton, W.A. (2000). Col2-GFP reporter marks chondrocyte lineage and chondrogenesis during mouse skeletal development. Dev. Dyn. *218*, 394–400.

Hagman, J., Belanger, C., Travis, A., Turck, C.W., and Grosschedl, R. (1993). Cloning and functional characterization of early B-cell factor, a regulator of lymphocyte-specific gene expression. Genes Dev. *7*, 760–773.

Hill, T.P., Spater, D., Taketo, M.M., Birchmeier, W., and Hartmann, C. (2005). Canonical Wnt/β-catenin signaling prevents osteoblasts from differentiating into chondrocytes. Dev. Cell *8*, 727–738.

Jochum, W., David, J.P., Elliott, C., Wutz, A., Plenk, H., Jr., Matsuo, K., and Wagner, E.F. (2000). Increased bone formation and osteosclerosis in mice overexpressing the transcription factor Fra-1. Nat. Med. *6*, 980–984.

Karsenty, G., and Wagner, E.F. (2002). Reaching a genetic and molecular understanding of skeletal development. Dev. Cell *4*, 389–406.

Kenner, L., Hoebertz, A., Beil, T., Keon, N., Karreth, F., Eferl, R., Scheuch, H., Szremska, A., Amling, M., Schorpp-Kistner, M., et al. (2004). Mice lacking JunB are osteopenic due to cell-autonomous osteoblast and osteoclast defects. J. Cell Biol. *164*, 613–623.

Kitazawa, R., Kitazawa, S., and Maeda, S. (1999). Promoter structure of mouse RANKL/TRANCE/OPGL/ODF gene. Biochim. Biophys. Acta *1445*, 134–141.

Komori, T., Yagi, H., Nomura, S., Yamaguchi, A., Sasaki, K., Deguchi, K., Shimizu, Y., Bronson, R.T., Gao, Y.H., Inada, M., et al. (1997).

Targeted disruption of Cbfa1 results in a complete lack of bone formation owing to maturational arrest of osteoblasts. Cell *89*, 755–764.

Kong, Y.Y., Yoshida, H., Sarosi, I., Tan, H.L., Timms, E., Capparelli, C., Morony, S., Oliveira-dos-Santos, A.J., Van, G., Itie, A., et al. (1999). OPGL is a key regulator of osteoclastogenesis, lymphocyte development and lymph-node organogenesis. Nature *397*, 315–323.

Lacey, D.L., Timms, E., Tan, H.L., Kelley, M.J., Dunstan, C.R., Burgess, T., Elliott, R., Colombero, A., Elliott, G., Scully, S., et al. (1998). Osteoprotegerin ligand is a cytokine that regulates osteoclast differentiation and activation. Cell *93*, 165–176.

Lagasse, E., and Weissman, I.L. (1997). Enforced expression of Bcl-2 in monocytes rescues macrophages and partially reverses osteopetrosis in op/op mice. Cell *89*, 1021–1031.

Lin, H., and Grosschedl, R. (1995). Failure of B-cell differentiation in mice lacking the transcription factor EBF. Nature *376*, 263–267.

Maier, H., Ostraat, R., Gao, H., Fields, S., Shinton, S.A., Medina, K.L., Ikawa, T., Murre, C.M., Singh, H., Hardy, R., and Hagman, J. (2004). Early B cell factor cooperates with Runx1 and mediates epigenetic changes associated with mb-1 transcription. Nat. Immunol. *5*, 1069–1077.

Malgaretti, N., Pozzoli, O., Bosetti, A., Corradi, A., Ciarmatori, S., Panigada, M., Bianchi, M.E., Martinez, S., and Consalez, G.G. (1997). Mmot1, a new helix-loop-helix transcription factor gene displaying a sharp expression boundary in the embryonic mouse brain. J. Biol. Chem. *272*, 17632–17639.

Mella, S., Soula, C., Morello, D., Crozatier, M., and Vincent, A. (2004). Expression patterns of the coe/ebf transcription factor genes during chicken and mouse limb development. Gene Expr. Patterns *4*, 537–542.

Nakashima, K., Zhou, X., Kunkel, G., Zhang, Z., Deng, J.M., Behringer, R.R., and de Crombrugghe, B. (2002). The novel zinc finger-containing transcription factor osterix is required for osteoblast differentiation and bone formation. Cell *108*, 17–29.

Notoya, M., Otsuka, E., Yamaguchi, A., and Hagiwara, H. (2004). Runx-2 is not essential for the vitamin D-regulated expression of RANKL and osteoprotegerin in osteoblastic cells. Biochem. Biophys. Res. Commun. *324*, 655–660.

Olsen, B.R., Reginato, A.M., and Wang, W. (2000). Bone development. Annu. Rev. Cell Dev. Biol. *16*, 191–220.

Otto, F., Thornell, A.P., Crompton, T., Denzel, A., Gilmour, K.C., Rosewell, I.R., Stamp, G.W., Beddington, R.S., Mundlos, S., Olsen, B.R., et al. (1997). *Cbfa1*, a candidate gene for cleidocranial dysplasia syndrome, is essential for osteoblast differentiation and bone development. Cell *89*, 765–771.

Simonet, W.S., Lacey, D.L., Dunstan, C.R., Kelley, M., Chang, M.S., Luthy, R., Nguyen, H.Q., Wooden, S., Bennett, L., Boone, T., et al. (1997). Osteoprotegerin: a novel secreted protein involved in the regulation of bone density. Cell *89*, 309–319.

Smith, E.M., Akerblad, P., Kadesch, T., Axelson, H., and Sigvardsson, M. (2005). Inhibition of EBF function by active Notch signaling reveals a novel regulatory pathway in early B-cell development. Blood *106*, 1995–2001.

Starr, D.B., Matsui, W., Thomas, J.R., and Yamamoto, K.R. (1996). Intracellular receptors use a common mechanism to interpret signaling information at response elements. Genes Dev. *10*, 1271–1283.

Takahashi, N., Akatsu, T., Udagawa, N., Sasaki, T., Yamaguchi, A., Moseley, J.M., Martin, T.J., and Suda, T. (1988). Osteoblastic cells are involved in osteoclast formation. Endocrinology *123*, 2600–2602.

Takayanagi, H., Kim, S., Koga, T., Nishina, H., Isshiki, M., Yoshida, H., Saiura, A., Isobe, M., Yokochi, T., Inoue, J., et al. (2002a). Induction and activation of the transcription factor NFATc1 (NFAT2) integrate RANKL signaling in terminal differentiation of osteoclasts. Dev. Cell *3*, 889–901.

Takayanagi, H., Kim, S., Matsuo, K., Suzuki, H., Suzuki, T., Sato, K., Yokochi, T., Oda, H., Nakamura, K., Ida, N., et al. (2002b). RANKL maintains bone homeostasis through c-Fos-dependent induction of interferon-β. Nature *416*, 744–749.

Teitelbaum, S.L. (2000). Bone resorption by osteoclasts. Science *289*, 1504–1508.

Teitelbaum, S.L., and Ross, F.P. (2003). Genetic regulation of osteoclast development and function. Nat. Rev. Genet. *4*, 638–649.

Thirunavukkarasu, K., Halladay, D.L., Miles, R.R., Yang, X., Galvin, R.J., Chandrasekhar, S., Martin, T.J., and Onyia, J.E. (2000). The osteoblast-specific transcription factor Cbfa1 contributes to the expression of osteoprotegerin, a potent inhibitor of osteoclast differentiation and function. J. Biol. Chem. *275*, 25163–25172.

Thirunavukkarasu, K., Miles, R.R., Halladay, D.L., Yang, X., Galvin, R.J., Chandrasekhar, S., Martin, T.J., and Onyia, J.E. (2001). Stimulation of osteoprotegerin (OPG) gene expression by transforming growth factor-β (TGF-β). Mapping of the OPG promoter region that mediates TGF-β effects. J. Biol. Chem. *276*, 36241–36250.

Tondravi, M.M., McKercher, S.R., Anderson, K., Erdmann, J.M., Quiroz, M., Maki, R., and Teitelbaum, S.L. (1997). Osteopetrosis in mice lacking haematopoietic transcription factor PU.1. Nature *386*, 81–84.

Travis, A., Hagman, J., Hwang, L., and Grosschedl, R. (1993). Purification of early-B-cell factor and characterization of its DNA-binding specificity. Mol. Cell. Biol. *13*, 3392–3400.

Tsurukai, T., Udagawa, N., Matsuzaki, K., Takahashi, N., and Suda, T. (2000). Roles of macrophage-colony stimulating factor and osteoclast differentiation factor in osteoclastogenesis. J. Bone Miner. Metab. *18*, 177–184.

Wang, S.S., Lewcock, J.W., Feinstein, P., Mombaerts, P., and Reed, R.R. (2004). Genetic disruptions of O/E2 and O/E3 genes reveal involvement in olfactory receptor neuron projection. Development *131*, 1377–1388.

Yasuda, H., Shima, N., Nakagawa, N., Yamaguchi, K., Kinosaki, M., Mochizuki, S., Tomoyasu, A., Yano, K., Goto, M., Murakami, A., et al. (1998). Osteoclast differentiation factor is a ligand for osteoprotegerin/osteoclastogenesis-inhibitory factor and is identical to TRANCE/RANKL. Proc. Natl. Acad. Sci. USA *95*, 3597–3602.

Yoshida, H., Hayashi, S., Kunisada, T., Ogawa, M., Nishikawa, S., Okamura, H., Sudo, T., and Shultz, L.D. (1990). The murine mutation osteopetrosis is in the coding region of the macrophage colony stimulating factor gene. Nature *345*, 442–444.